PROCEEDINGS OF SPIE

SPIEDigitalLibrary.org/conference-proceedings-of-spie

Identifying the optical phenomena responsible for the blue appearance of veins

Spencer R. Van Leeuwen
Gladimir V. G. Baranoski

SPIE.

Identifying the Optical Phenomena Responsible for the Blue Appearance of Veins

Spencer R. Van Leeuwen[1] and Gladimir V. G. Baranoski[1]

[1]Natural Phenomena Simulation Group, School of Computer Science, University of Waterloo, 200 University Avenue, Waterloo, Ontario, Canada N2L 3G1

ABSTRACT

Blue in nature is often associated with beauty. It can be observed all around us, from captivating blue eyes to iridescent blue butterfly wings. While colours in nature are often the result of pigmentation, the majority of natural blue is produced by structural coloration. The colour of the sky, for example, is primarily caused by Rayleigh scattering. In this paper, we examine a single occurrence of blue in nature, specifically the blue appearance of veins near the surface of human skin. The most comprehensive investigation of this coloration to date showed that it arises from a combination of the scattering properties of skin and the absorptance of venous blood. However, that work only considered broad optical properties of these mediums and did not identify the source of the colour. In this paper, we employ *in silico* experiments, performed using first-principles light interaction models for skin and blood, to investigate the net effect of skin and vein optical properties on their aggregate reflectance across the visible range. We show that the contribution of skin to the distinct appearance of veins primarily results from Rayleigh scattering occurring within the papillary dermis, a sublayer of the skin. The results of this paper, in addition to addressing an old open scientific question, may have practical implications for performing non-invasive measurements of the physiological properties of skin and blood.

Keywords: skin, blood, vein, reflectance, Rayleigh scattering, predictive simulation

1. INTRODUCTION

Complex optical phenomena can often lead to counterintuitive material appearances. Such is the case for the appearance of veins (Figure 1). While the colour of skin and venous blood are both not blue, for some reason their combination results in what we might call a bluish appearance. The word "bluish" is used in scientific literature to describe skin tones that appear subjectively blue. Bluish skin tones, such as those caused by subcutaneous veins, may appear closer to grey than blue and do not have a specific quantitative characterization. Accordingly, the results presented in this paper are primarily visual to allow for a qualitative assessment of appearance.

Kienle *et al.*[1] suggest that several factors contribute to the bluish appearance of veins. Blue light does not penetrate as deeply into the skin as red light. Accordingly, although blood absorbs blue light more strongly than red, a higher percentage of red light reaches the vein itself, resulting in more red light being absorbed overall. They suggest that these considerations combined with human perceptual phenomena provide an explanation for the bluish appearance of veins. These observations, however, only refer to the broad optical properties of skin and blood. In this paper, we explore the optical properties of the materials composing skin and blood. In particular, we examine their distinct light attenuation (absorbing and scattering) capabilities in the visible domain.

Rayleigh scattering is the scattering of light by structures smaller in magnitude than the wavelength of the affected light. It is a wavelength-dependent phenomenon that affects shorter wavelengths more strongly than longer wavelengths.[2,3] In the early investigation of skin optical properties, it was suggested by Edwards and Duntley[4] that Rayleigh scattering in the epidermis might be responsible for the bluish appearance of veins. More recently, Anderson and Parrish[5] observed that since the ratio of diffuse transmittance to direct transmittance

Further author information: (Send correspondence to Gladimir V. G. Baranoski)
Gladimir V. G. Baranoski: E-mail: gvgbaran@cs.uwaterloo.ca

Light in Nature VI, edited by Joseph A. Shaw, Katherine Creath, Vasudevan Lakshminarayanan,
Proc. of SPIE Vol. 10367, 103670F · © 2017 SPIE · CCC code: 0277-786X/17/$18
doi: 10.1117/12.2274560

Figure 1. Photograph illustrating the distinct contrast of skin appearance caused by subcutaneous veins.

in the stratum corneum and epidermis is primarily wavelength-independent, there is not a significant amount of Rayleigh scattering in these tissues. Alternatively, they suggest that scattering in the dermis is stronger for shorter wavelengths. In order to develop a model for scattering in the dermis, Jacques[6] used Mie theory to approximate the scattering of collagen fiber bundles. He found that considering Rayleigh scattering in addition to large-scale scattering provided a good agreement with scattering behaviour in the dermis. He speculated that the fibrils composing the microstructure of the collagen fiber bundles could potentially be a source of this Rayleigh scattering.

Recently, Baranoski *et al.*[7] employed these observations to perform an *in silico* investigation showing that it is necessary to consider Rayleigh scattering in the papillary dermis in order to explain the bluish or purple appearance of cyanotic fingertips. More specifically, they used measured radius values for the fibrils present in the papillary dermis, obtained by Arao *et al.*,[8] to show that it is necessary to consider Rayleigh scattering in this tissue in order to elicit the characteristic hues of cyanotic skin. In this paper, we use a similar approach to show that Rayleigh scattering in the papillary dermis is primarily responsible for the skin's contribution to the bluish appearance of veins.

Our investigation involved *in silico* experiments performed using first-principles light interaction models for skin and blood. These models are known as HyLIoS[9] (*Hy*perspectral *L*ight *I*mpingement *o*n *S*kin) and CLBlood[10,11] (*C*ell-Based *L*ight Interaction Model for Human *Blood*), respectively, and they account for all significant light-attenuating materials in the skin and blood. The use of an *in silico* framework in our investigation allowed for highly controlled and reproducible experiments considering a specific specimen characterization. It also made it possible to disable Rayleigh scattering in the papillary dermis and assess this phenomenon's effect on the appearance of veins. This procedure would likely be complicated or impossible to perform *in situ* without affecting other optical properties of the skin.

The remainder of this paper is organized as follows. In Section 2, we discuss light attenuation processes that occur within the skin and blood in the visible domain (400-700 nm). This will serve as a foundation for our investigation and discussion. Next, in Section 3, we discuss the models employed in this investigation and how they were combined to simulate the optical properties of skin with a subcutaneous vein. We then outline our *in silico* experimental setup in Section 4, present our results in Section 5, and discuss their implications in Section 6. In Section 7, we provide a brief conclusion and potential directions for future work.

2. BIOPHYSICAL BACKGROUND

In this section, we describe the tissues relevant to the appearance of veins. For each tissue, we outline the constituent materials that contribute significantly to the tissue's attenuation of light in the visible domain. Measured absorptance data for each pigment discussed in this section is presented in Figure 2. We also discuss the role of the detour effect and the sieve effect in the optical properties of skin and blood.

2.1 Skin

Human skin can be divided into three distinct layers. From outermost to innermost, they are the stratum corneum, epidermis and dermis.[12] The epidermis can be further subdivided into the stratum granulosum, stratum spinosum and stratum basale.

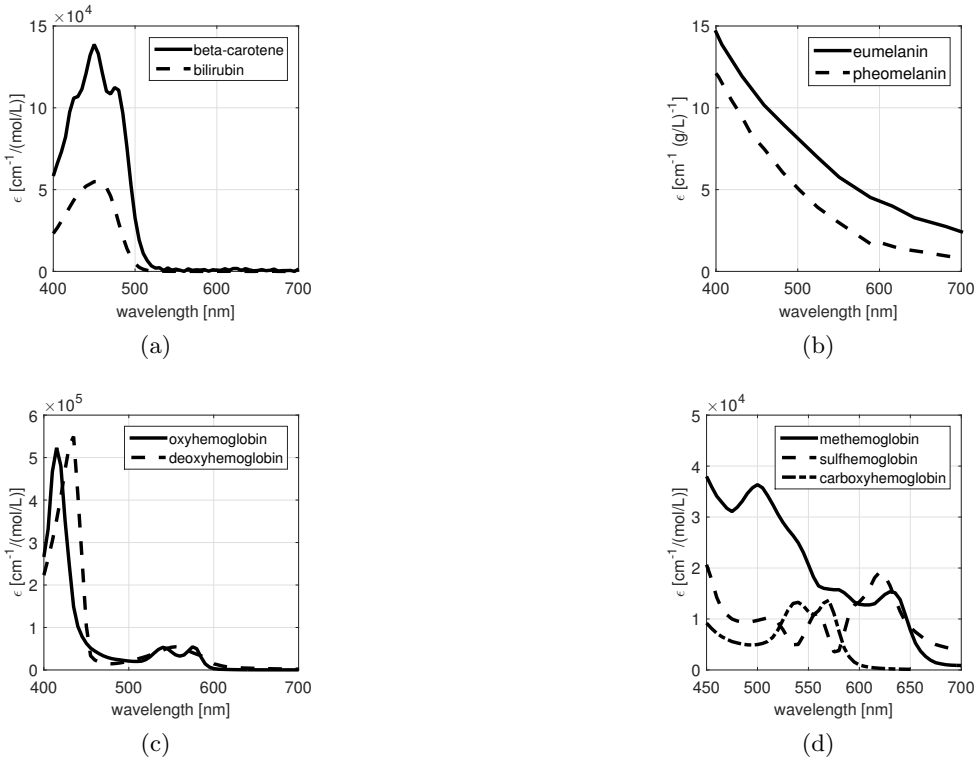

Figure 2. Absorption data for skin and blood components with a significant impact on light attenuation in the visible domain. (a) Molar extinction coefficient curves for beta-carotene and bilirubin.[21] (b) Extinction coefficient curves for melanin.[22] (c) Molar extinction coefficient curves for functional hemoglobins.[23] (d) Molar extinction coefficient curves for dysfunctional hemoglobins.[24–26]

The absorption of light traversing the stratum corneum and epidermis is dominated by melanin with a minor contribution from beta-carotene (Figure 2(a)).[13] Melanin is synthesized and preferentially concentrated in the stratum basale.[14] Melanin can be classified as either brown-black eumelanin or yellow-red pheomelanin (Figure 2(b)), the former of which has a significantly higher concentration in skin. Melanin can be dispersed throughout the epidermis in colloidal form or clustered within melanosomes.[15]

In the skin, light is mostly scattered by heterogeneous structures such as cells, organelles and fibers.[13] In the stratum corneum and epidermis, scattering is predominantly wavelength-independent and forward-scattering.[5] Scattering in the epidermis is dominated by melanosomes[16] which can be described as particles with the shape of a prolate spheroid[17] and a melanin concentration of 17.9% to 72.4%.[16] In lightly pigmented specimens, melanosomes can occur in a group surrounded by a transparent membrane, known as a melanosome complex.[17,18]

The dermis can be subdivided into two layers. The outermost layer, the papillary dermis, is composed of loosely-packed reticulin and collagen fibers which, in turn, are composed of smaller-sized fibrils. Since these fibrils are smaller in magnitude than wavelengths of light within the visible spectrum, any scattering caused by these structures would follow the Rayleigh scattering theory. The innermost layer, the reticular dermis, is composed of dense connective tissue. A network of blood vessels also runs throughout the dermis with wider vessels in the reticular dermis. Blood-borne pigments within these vessels (Figure 2(b)-(d)) dominate the dermis's absorptance in the visible domain.[19] Furthermore, diffusion of red light traversing the dermis[20] is likely caused by large-scale, wavelength-independent scattering by the dense connective tissues and wider vessels in the reticular dermis. Since this scattering is strong enough to diffuse the light, it would probably dominate any Rayleigh scattering that may occur in the reticular dermis.

2.2 Blood

Blood is primarily composed of plasma and red (blood) cells.[27] A red cell consists of a thin membrane encapsulating a hemoglobin solution. The attenuation of light by red cells exceeds that of other blood components by 2-3 orders of magnitude.[27] The absorptance of red cells in the visible domain is primarily attributed to hemoglobins (Figure 2(c) and (d)) and the scattering behaviour is determined by the red cells' shape and orientation.[28] Both the properties of the plasma and the platelets it contains amplify the scattering achieved by red cells.[27,29]

The distribution of red cell orientations in blood can change depending on the shear rate of the sample (*i.e.*, the velocity gradient in the direction normal to the flow).[30] At low, intermediate and high shear rates, the red cells are predominantly randomly oriented, rolling or aligned with the flow direction, respectively.[30] When the volume fraction of the blood occupied by red cells, known as hematocrit, is above 40%, the alignment of the cells becomes more pronounced.

2.3 Hypodermis

The hypodermis is a layer immediately below the skin composed of fat-containing adipose tissue. Due to its low absorptance, the majority of visible light that penetrates the hypodermis is scattered by its large cellular structures and remitted into the reticular dermis.[12]

2.4 Vein Wall

The vein wall is composed of elastin, collagen and muscle tissue.[31] The absorption of visible light within the vein wall is dominated by hemoglobin in the muscle tissue (Figure 2(c) and (d)).[32] It is also possible that light traversing the vein wall may be scattered by heterogeneous structures, similar to scattering in the skin.

2.5 Detour and Sieve Effects

Skin and blood are both turbid mediums characterized by their heterogeneously-distributed, pigment-containing structures. These structures are melanosomes and red cells, respectively. When light traverses a turbid medium, scattering by these structures can increase the optical path length which results in an increase in the probability of absorption. Conversely, the light may not encounter any pigment-containing structure and, therefore, have a minimal chance of absorption. These phenomena are respectively known as the detour effect[33] and the sieve effect.[34] Their combined contribution to the overall absorptance of a turbid medium depends on the properties and distribution of the medium's pigment-containing structures.

3. EXPERIMENTAL FRAMEWORK

3.1 Model Background and Setup

In our *in silico* experiments, we use HyLIoS and CLBlood to simulate the interaction of light with skin and the blood flowing through the subcutaneous vein, respectively. These first-principles models employ measured optical properties of constituent materials to govern the attenuation of light. Although this paper is focused on light in the visible domain, both models consider all constituent materials with a significant contribution to light attenuation in the ultraviolet, visible and infrared domains. Measured optical properties for these materials were obtained from scientific literature and made available on our website.[35,36] References to this data can also be found in the models' original publications.[9,10] Additionally, HyLIoS and CLBlood account for sieve and detour effects by individually distributing melanosomes throughout the epidermis and red cells throughout the plasma, respectively. This includes the grouping of melanosomes within melanosome complexes. Both of these models have been evaluated quantitatively and qualitatively against measured data in their original publications.[9,10] CLBlood was also updated and re-evaluated in a following technical report.[11]

In our experiments, we obtained simulated reflectance measurements for skin specimens with and without a subcutaneous vein. For a skin specimen without a subcutaneous vein, we use the HyLIoS model as described in its original publication. In particular, it has a layer below the reticular dermis that represents the hypodermis and reflects light diffusely back into the reticular dermis with 100% probability. For a skin specimen with a subcutaneous vein, light that reaches the bottom of the skin will either be diffusely reflected or absorbed by the vein. The probability of either event occurring is precomputed for a shorter experimental runtime (Section 4.2).

3.2 Vein Representation

We use a three layer model to represent the vein. The first and third layers represent the vein wall and the second layer employs CLBlood to represent flowing venous blood. When light encounters a layer boundary, a Fresnel test[13] is performed to determine whether the light is reflected or transmitted.

The refractive index selected for the vein wall is 1.39, which corresponds to a measured value for the vena femoralis.[37] Any light that is transmitted below the bottom vein wall layer is discarded. Note that this choice does not affect the overall reflectance of the skin specimen due to the low transmittance and high absorptance of the vein. We also do not consider any absorption or scattering of light within the vein wall. The implications of this simplification will be addressed in Section 6.1.

4. IN SILICO EXPERIMENTAL SETUP

In our experiments, we obtained directional-hemispherical reflectance curves for various skin specimens with a virtual spectrophotometer[38] considering a 5° angle of incidence. Seeing as the employed models are formulated using a Monte Carlo approach, we performed the experiments considering 10^6 samples per wavelength with a 5 nm spectral resolution. We then used the computed reflectance data to generate textured colour swatches representing the appearance of the skin specimen considering a given illuminant.

In the first set of experiments, we computed reflectance curves for the baseline skin specimen with and without a subcutaneous vein (Figure 5(a)). Corresponding reflectance curves were computed without considering Rayleigh scattering in the skin (Figure 5(b)). For each pair of reflectance curves, we generated several swatches considering distinct illuminants (Figure 6).

In the second set of experiments, we varied the concentration of blood and melanin in the skin. We performed experiments for each specimen with and without considering Rayleigh scattering. For each experiment, we generated a swatch representing skin with a vein running down the center, considering a D65 illuminant (Figure 7).

In the following subsections, we discuss the characterization of skin specimens, the precomputation of the vein's reflectance, the process of disabling Rayleigh scattering and the online reproducibility of our experiments.

4.1 Skin Specimens

In our experiments, we consider a lightly pigmented skin specimen with various levels of cutaneous pigmentation and dermal blood content. In our first set of experiments (Figures 5 and 6), we consider a baseline skin specimen characterized by the parameters in Tables 1 and 2. Accompanying each parameter value is a list of references that provide its physiological basis.

For the additional skin specimens considered in the second set of experiments (Figure 7), we multiply the melanin and blood parameters in Table 2 by $f_{mel} \in \{1.0, 1.5, 2.0, 2.5\}$ and $f_{bl} \in \{1.0, 1.5, 2.0, 2.5\}$, respectively. For each experiment, the mean epidermal melanin content is in the range 1-3% and dermal blood content is in the range 2-6%, corresponding to the physiological characterization of a lightly pigmented specimen.[39]

4.2 Vein Precomputation

Since we know that visible light is diffused by the dermis,[20] we can assume a uniform distribution for the angle of incidence of light that encounters the vein. This assumption allows us to precompute the probability that light is reflected by the vein using the representation outlined in Section 3.2. To obtain this probability, we first computed its reflectance considering polar angles in $[0°, 90°)$ at each 5° interval and azimuthal angles in $[0°, 360°)$ at each 90° interval. For each angle of incidence, we considered the blood specimen characterization presented in Table 3 and 10^5 samples per wavelength. Since we assume that the light entering the vein is uniformly distributed, we then averaged the reflectance values across all samples at each wavelength (λ) to get the probability of light being reflected by the vein ($p^r_{vein}(\lambda)$), presented in Figure 3.

Table 1. HyLIoS parameters employed in the general characterization of all skin specimens considered in this investigation.

HyLIoS Parameters	Values	References
Aspect Ratio of Skin Surface Fold	0.1	[40, 41]
Stratum Corneum Thickness (cm)	0.0004	[42–45]
Stratum Granulosum Thickness (cm)	0.0033	[46]
Stratum Spinosum Thickness (cm)	0.0033	[46]
Stratum Basale Thickness (cm)	0.0033	[47]
Papillary Dermis Thickness (cm)	0.02	[5]
Reticular Dermis Thickness (cm)	0.125	[5]
Stratum Granulosum Melanosome Content (%)	0.0	[16, 39]
Stratum Spinosum Melanosome Content (%)	0.0	[16, 39]
Stratum Basale Melanosome Dimensions ($\mu m \times \mu m$)	0.41×0.17	[17]
Melanosome Eumelanin Concentration (mg/mL)	32.0	[48, 49]
Melanosome Pheomelanin Concentration (mg/mL)	2.0	[48, 49]
Dermal Oxyhemoglobin Fraction (%)	90.0	[50]
Hemoglobin Concentration in Blood (mg/mL)	147.0	[51, 52]
Methemoglobin Concentration in Blood (mg/mL)	1.5	[53]
Carboxyhemoglobin Concentration in Blood (mg/mL)	1.5	[54]
Sulfhemoglobin Concentration in Blood (mg/mL)	0.0	[26]
Blood Bilirubin Concentration (mg/mL)	0.003	[55]
Stratum Corneum Beta-carotene Concentration (mg/mL)	2.1E-4	[56]
Epidermis Beta-carotene Concentration (mg/mL)	2.1E-4	[56]
Blood Beta-carotene Concentration (mg/mL)	7.0E-5	[56]
Stratum Corneum Water Content (%)	35.0	[57, 58]
Epidermis Water Content (%)	60.0	[57, 59]
Papillary Dermis Water Content (%)	75.0	[57, 59]
Reticular Dermis Water Content (%)	75.0	[57, 59]
Stratum Corneum Lipid Content (%)	20.0	[60]
Epidermis Lipid Content (%)	15.1	[57, 61, 62]
Papillary Dermis Lipid Content (%)	17.33	[57, 61, 62]
Reticular Dermis Lipid Content (%)	17.33	[57, 61, 62]
Stratum Corneum Keratin Content (%)	65.0	[47, 63, 64]
Stratum Corneum Urocanic Acid Density (mol/L)	0.01	[65]
Skin DNA Density (mg/mL)	0.185	[57, 66, 67]
Stratum Corneum Refractive Index	1.55	[68, 69]
Epidermis Refractive Index	1.4	[68, 70]
Papillary Dermis Refractive Index	1.39	[20, 68]
Reticular Dermis Refractive Index	1.41	[20, 68]
Melanin Refractive Index	1.7	[71]
Papillary Dermis Scatterers' Refractive Index	1.53	[72]
Radius of Papillary Dermis Scatterers (nm)	40.0	[8]
Papillary Dermis Fraction Occupied by Scatterers (%)	22.0	[6]

Table 2. HyLIoS melanin and blood content parameters that are modified to produce different skin specimen characterizations. The presented values correspond to the baseline skin specimen. The melanin parameters* and blood parameters† are multiplied by a factor of f_{mel} and f_{bl}, respectively, to provide the skin specimens in the second set of experiments.

HyLIoS Parameters	Values	References
Stratum Basale Melanosome Content (%)	1.0 *	16, 39
Stratum Granulosum Colloidal Melanin Content (%)	0.5 *	15, 16, 73
Stratum Spinosum Colloidal Melanin Content (%)	0.5 *	15, 16, 73
Stratum Basale Colloidal Melanin Content (%)	0.5 *	15, 16, 73
Papillary Dermis Blood Content (%)	0.2 †	6, 52
Reticular Dermis Blood Content (%)	0.2 †	6, 52

Table 3. CLBlood parameters employed in the characterization of flowing venous blood.

CLBlood Parameters	Values	References
Hematocrit (%)	45	74, 75
Sample thickness (μm)	1270.0	76
Randomly oriented cells (%)	10	30, 77, 78
Rolling oriented cells (%)	60	30, 77, 78
Aligned oriented cells (%)	30	30, 77, 78
Oxyhemoglobin (%)	67.9	79
Deoxyhemoglobin (%)	29.1	79
Sulfhemoglobin (%)	0	80
Methemoglobin (%)	1.5	81
Carboxyhemoglobin (%)	1.5	82
Mean cell hemoglobin content (g/L)	330.0	74

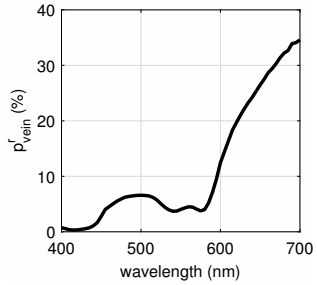

Figure 3. The precomputed probability of light being reflected by the subcutaneous vein specimen (p^r_{vein}) employed in our experiments. This curve was computed using the procedure outlined in Section 4.2

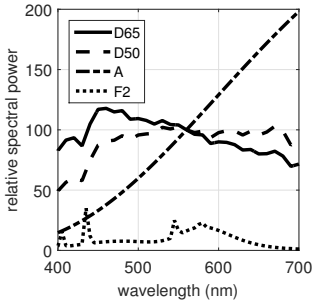

Figure 4. Relative spectral power distribution of each CIE standard illuminant[84] employed in the swatch generation process.

4.3 Disabling Rayleigh Scattering

In HyLIoS, the amount of wavelength-dependent Rayleigh scattering in the papillary dermis is controlled by the following Rayleigh scattering coefficient:[9,83]

$$\mu_s^R(\lambda) = \frac{32\pi^4 r^3 v_s}{\lambda^4} \left(\frac{\eta^2 - 1}{\eta^2 + 1} \right)^2, \tag{1}$$

where r and v_s represent the radius and volume of the scatterers. The variable η is the ratio between the refractive index of the scatterers (η_s) and the refractive index of the papillary dermis (η_{pd}). To deactivate Rayleigh scattering, we simply set $\eta_s = \eta_{pd}$ which results in $\mu_s^R = 0$. The values for r, v_s, η_{pd} and the default value for η_s are given in Table 1.

4.4 Swatch Generation

Swatches are used in this investigation to approximate the appearance of a given skin specimen under distinct illumination conditions. To generate the colour of a swatch, the skin specimen's calculated reflectance curve is convoluted with a selected illuminant's relative spectral power distribution and the broad spectral response of the human photoreceptors.[84] The last step involves a standard XYZ to sRGB conversion procedure[85] which includes a white balancing calculation considering the selected illuminant. In our investigation, we considered four standard CIE illuminants whose relative spectral power distributions are presented in Figure 4. D50 and D65 approximate daylight at different times of day, A is an incandescent light, and F2 is a "cool white fluorescent" light typical of an office environment.[84] Since F2 was measured separately from the other illuminants and the provided data is in relative units, we decided to increase its intensity in the swatch generation process to get a similar qualitative brightness across the swatches. After generating the colour, we use a greyscale texture to vary the colour across each swatch to make them appear more realistic.

4.5 Online Reproducibility

The experiments in this paper can be reproduced with our online version of HyLIoS[86] which is deployed using our custom model distribution system.[87] This system allows a user to perform their own experiments with a specified skin specimen characterization and experimental setup. In order to reproduce the reflectance of skin with a subcutaneous vein, we have included options to enable the vein and select a precomputed vein specimen. Additionally, we have made it possible to reproduce venous reflectance from a single angle of incidence using our online version of CLBlood.[88]

5. RESULTS

For our first set of experimental results, we explore the effect of disabling Rayleigh scattering in the skin on the appearance of the vein. For comparison purposes, all results considering a subcutaneous vein are accompanied by results for the same skin specimen without the vein.

(a) (b)

Figure 5. Modeled reflectance curves obtained for the baseline skin specimen with and without a subcutaneous vein. (a) With Rayleigh scattering. (b) Without Rayleigh scattering.

First, we examine the reflectance results in Figure 5. Comparing the two reflectance curves computed considering Rayleigh scattering, presented in Figure 5(a), reveals a smaller difference between them in the shorter (blue) wavelength range. In particular, the difference between the two curves is negligible in the region near 400 nm. Given the near zero probability of light reflected by the vein in this region (Figure 3), the light must be scattered out of the skin before it reaches the vein.

This behaviour could potentially be attributed to Rayleigh scattering, so let us examine Figure 5(b). We can observe that disabling Rayleigh scattering reduces the reflectance significantly in both samples in the region near 400 nm. Furthermore, the plot shows that the amount of reflected light in this region is lower for the skin specimen with a subcutaneous vein. This indicates that the absence of Rayleigh scattering allows more light to reach the vein. To support this claim, we remark that the shape of the reflectance curve computed for the skin specimen with a subcutaneous vein more closely resembles the probability of light being reflected by the vein itself (Figure 3).

Now, let us examine the generated swatches in Figure 6 to see how these results translate to appearance. In Figure 6(a), we present swatches corresponding to the data presented in Figure 5(a) considering several illumination conditions. The colours depicted in these swatches generally match our expectations for the appearance of skin with and without a subcutaneous vein. Conversely, the reflectance data in Figure 5(b), computed without considering Rayleigh scattering, yields a blood-like swatch colour for the skin specimen with a subcutaneous vein which can be observed in Figure 6(b).

Swatches belonging to our second set of experimental results are presented in Figure 7. It is clear that the role of Rayleigh scattering in the appearance of a skin specimen with a subcutaneous vein is consistent across all considered skin characterizations.

6. DISCUSSION

The first set of experimental results demonstrates that Rayleigh scattering plays an integral role in the appearance of veins. The second set shows that varying blood and melanin content within the range of physically plausible concentrations for a lightly pigmented specimen[39] does not have a large effect on the vein's appearance. An examination of relevant pigments in the skin (Figure 2) reveals that none of them absorb long (red) wavelengths more strongly than short (blue) wavelengths. Therefore, we can attribute the bluish appearance of veins to Rayleigh scattering in the papillary dermis and the strong absorptance of hemoglobins in the venous blood's red cells.

In the following subsections, we discuss additional considerations regarding our assumptions and the interpretation of our results.

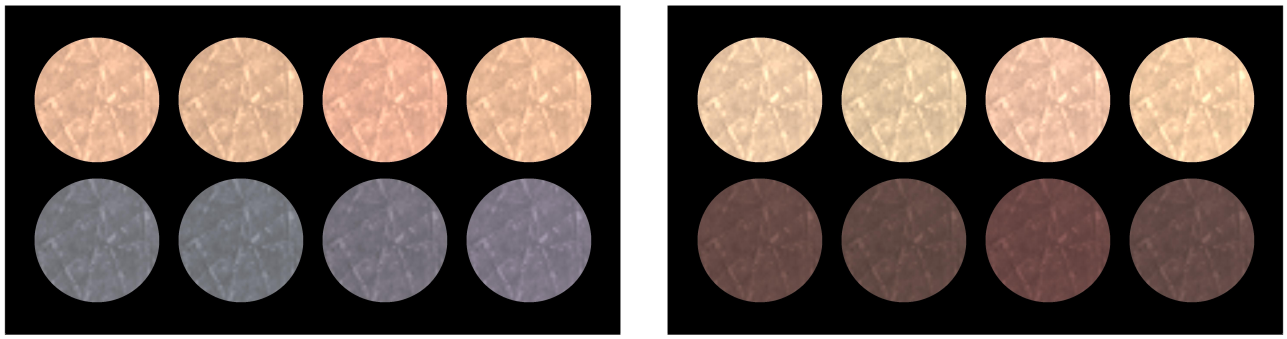

(a) (b)

Figure 6. Swatches generated for the baseline skin specimen to illustrate the effect of Rayleigh scattering in the papillary dermis. For comparison purposes, we present swatches for specimens with (bottom) and without (top) a subcutaneous vein. The swatches were generated using the procedure described in Section 4.4. From left to right, the swatches in each subfigure were generated considering CIE standard illuminants D50, D65, A and F2. (a) With Rayleigh scattering. (b) Without Rayleigh scattering.

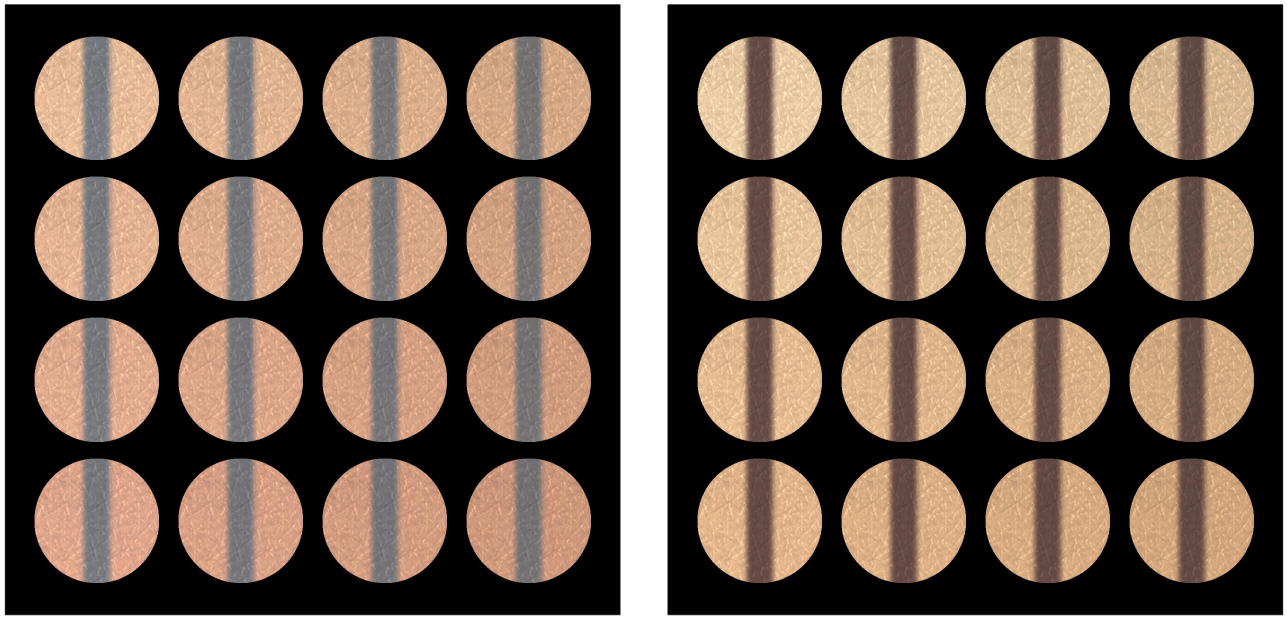

(a) (b)

Figure 7. Generated swatches depicting a skin specimen with a subcutaneous vein running down the middle. The swatches were generated using the procedure described in Section 4.4 considering the D65 illuminant. Distinct skin specimens were obtained by multiplying melanin and blood content (Table 2) by f_{mel} and f_{bl}, respectively. Left to right: $f_{mel} = 1.0, 1.5, 2.0, 2.5$. Top to bottom: $f_{bl} = 1.0, 1.5, 2.0, 2.5$. (a) With Rayleigh scattering. (b) Without Rayleigh scattering.

6.1 Intermediate Tissues

In our experiments, we do not consider any adipose tissue between the skin and the vein. In the human body, if a vein is deep enough, then scattering in the adipose tissue ensures that the vein is not visible. Accordingly, a less visually prominent vein may have a thin layer of adipose tissue between itself and the skin. We also do not consider the light attenuating properties of the vein wall. We remark that although these considerations may have an effect on the quantitative results, we believe that neither of these tissues can be the primary source of the distinct appearance of veins.

The weak absorption of visible light in these tissues is dominated by hemoglobin[12,31,32] which has a significantly higher concentration in the venous blood. If we were to consider the effect of hemoglobin in these tissues on the overall reflectance of a skin specimen with a subcutaneous vein, it would be similar to increasing the hemoglobin concentration in the reticular dermis. As we can see in Figure 7, this does not have a significant effect on the bluish appearance of the vein.

There is also a possibility that small heterogeneous structures in these tissues produce Rayleigh scattering. However, our experiments indicate that Rayleigh scattering in the skin is strong enough to elicit the bluish appearance of veins. This is corroborated by the fact that cyanotic fingertips would not appear bluish if Rayleigh scattering in the papillary dermis was not sufficient to prevent blue light from reaching the reticular dermis.[7] Since Rayleigh scattering in the skin occurs before light reaches the hypodermis or vein wall, any additional Rayleigh scattering in these subcutaneous tissues could only increase the, already sufficient, remittance of blue light.

6.2 Blood Parameters

We performed several additional experiments, not presented in this paper, to assess the effect of varying the venous blood characterization. When experimenting with various oxygen saturation levels, we observed that an increase in oxygen made a skin specimen with a subcutaneous vein appear more purple and a decrease in oxygen made it appear more blue. This behaviour is consistent with observations by Kienle *et al.*[1] We also explored different distributions of red cell orientations in the flowing venous blood, corresponding to different shear rates. This did not noticeably affect the visual appearance of a skin specimen with a subcutaneous vein.

6.3 Comment on Vein Appearance

In this paper, we have been referring to the appearance of veins as bluish. We remark that a subcutaneous vein may also appear to be subjectively more green, purple, or grey than blue when considering different physiological or illumination conditions. It is important to note that Rayleigh scattering occurring in the papillary dermis would play a vital role in the appearance of any visible subcutaneous vein, even though its contribution may not always result in a dominantly blue appearance.

7. CONCLUSION AND FUTURE WORK

In this paper, we showed that Rayleigh scattering in the papillary dermis is responsible for the skin's contribution to the bluish appearance of veins. In particular, Rayleigh scattering in the papillary dermis remits blue light from the skin before it can reach the blood flowing through the subcutaneous vein. The hemoglobin contained within the venous blood's red cells then moderately absorbs the red light that reaches the vein. The combined effect of these two phenomena results in the distinct appearance of veins.

There are many possibilities for future work in this area. For example, Kienle *et al.*[1] mentioned that the optical depth of a subcutaneous vein and the oxygen saturation of its blood affect the skin's coloration. Adding adipose tissue to the framework described in this paper (Section 3) between the skin and the vein would make it possible to investigate the combined effect of these properties. Another possibility would be to evaluate the impact of the masking effect of melanosomes on the appearance of subcutaneous veins in moderately and darkly pigmented skin specimens. In addition to improving our understanding of fundamental optical mechanisms occurring within the skin, these investigations could aid in the design of non-invasive optical measurement devices aimed at the detection of physiological changes within the skin and subcutaneous veins. Furthermore,

since the models employed in this paper are hyperspectral, any future investigations employing the framework described in this paper could be performed in the ultraviolet, visible and infrared domains.

From a visual perspective, the addition of adipose tissue to the framework described in this paper and an exploration of other skin characterizations could enable the reproduction of the various skin tones caused by subcutaneous blood vessels. Additionally, placing the vein representation within the cutaneous tissues could be used to simulate the appearance of enlarged cutaneous vessels. These advancements could contribute to improved computer-generated representations of skin which would have practical implications for scientific, educational and entertainment applications requiring a realistic visualization of the human body.

REFERENCES

[1] Kienle, A., Lilge, L., Vitkin, I. A., Patterson, M. S., Wilson, B. C., Hibst, R., and Steiner, R., "Why do veins appear blue? A new look at an old question," *Applied Optics* **35**(7), 1151–1160 (1996).

[2] Strutt, J. W., "On the scattering of light by small particles," *Philosophical Magazine* **41**, 447–454 (June 1871).

[3] Strutt, J. W., "On the transmission of light through an atmosphere containing many small particles in suspension, and on the origin of the blue of the sky," *Philosophical Magazine* **47**, 375–384 (April 1899).

[4] Edwards, E. A. and Duntley, S. Q., "The pigments and color of living human skin," *American Journal of Anatomy* **65**(1), 1–33 (1939).

[5] Anderson, R. R. and Parrish, J. A., "The optics of human skin," *Invest Dermatol* **77**(1), 13–9 (1981).

[6] Jacques, S. L., "Origins of tissue optical properties in the UVA, visible, and NIR regions," *OSA TOPS on Adv. in Opt. Imaging and Photon Migration* **2**, 364–369 (1996).

[7] Baranoski, G. V. G., Van Leeuwen, S. R., and Chen, T. F., "Elucidating the biophysical processes responsible for the chromatic attributes of peripheral cyanosis," in [*39th Annual International Conference of the IEEE Engineering in Medicine and Biology Society (EMBC)*], (July 2017). In Press.

[8] Arao, H., Obata, M., Shimada, T., and Hagisawa, S., "Morphological characteristics of the dermal papillae in the development of pressure sores," *Journal of Tissues Viability* **8**(3), 17–23 (1998).

[9] Chen, T. F., Baranoski, G. V. G., Kimmel, B. W., and Miranda, E., "Hyperspectral modeling of skin appearance," *ACM Transactions on Graphics* **34**(3), 31:1–14 (2015).

[10] Yim, D., Baranoski, G. V. G., Kimmel, B. W., Chen, T. F., and Miranda, E., "A cell-based light interaction model for human blood," in [*Computer Graphics Forum*], **31**(2pt4), 845–854, Wiley Online Library (2012).

[11] Van Leeuwen, S. R., Baranoski, G. V. G., and Kimmel, B. W., "Revisiting the CLBlood model: Formulation enhancements and online deployment." Technical Report CS-2017-01, School of Computer Science, University of Waterloo (February 2017).

[12] Yang, M. F., Tuchin, V. V., and Yaroslavsky, A. N., "Principles of light-skin interactions," in [*Light-Based Therapies for Skin of Color*], Baron, E. D., ed., 1–44, Springer-Verlag, London (2009).

[13] Anderson, R. R. and Parrish, J. A., "Optical properties of human skin," in [*The Science of Photomedicine*], Regan, J. D. and Parrish, J. A., eds., 147–194, Plenun Press, N.Y., USA (1982).

[14] de Graaff, K. M. V., [*Human Anatomy*], W. C. Brown Publishers, Dubuque, IO, USA, 4th ed. (1995).

[15] Pathak, M. A., "Functions of melanin and protection by melanin," in [*Melanin: Its Role in Human Photoprotection*], L. Zeise, M. R. C. and Fitzpatrick, T. B., eds., 125–134, Valdenmar Publishing Co., Overland Park, Kansas, USA (1995).

[16] Kollias, N., Sayre, R. M., Zeise, L., and Chedekel, M. R., "Photoprotection by melanin," *J. Photoch. Photobio. B.* **9**(2), 135–60 (1991).

[17] Olson, R. L., Gaylor, J., and Everett, M. A., "Skin color, melanin, and erythema," *Arch. Dermatol.* **108**(4), 541–544 (1973).

[18] Szabo, G., Gerald, A., Pathak, M., and Fitzpatrick, T. B., "Racial differences in the fate of melanosomes in human epidermis," *Nature* **222**, 1081–1082 (06 1969).

[19] Jacquez, J. A., Huss, J., McKeehan, W., Dimitroff, J. M., and Kuppenhein, H. F., "Spectral reflectance of human skin in the region 0.7-2.6 μ," *J. Appl. Physiol.* **8**, 297–299 (1955).

[20] Jacques, S. L., Alter, C. A., and Prahl, S. A., "Angular dependence of HeNe laser light scattering by human dermis," *Lasers Life Sci.* **1**, 309–333 (1987).
[21] Prahl, S. A., "PhotochemCAD spectra by category," tech. rep., Oregon Medical Laser Center (2001).
[22] Jacques, S. L., "Optical absorption of melanin," tech. rep., Oregon Medical Laser Center (2001).
[23] Prahl, S. A., "Optical absorption of hemoglobin," tech. rep., Oregon Medical Laser Center (1999).
[24] Randeberg, L. L., Bonesrønning, J. H., Dalaker, M., Nelson, J. S., and Svaasand, L. O., "Methemoglobin formation during laser induced photothermolysis of vascular skin lesions," *Lasers in Surgery and Medicine* **34**(5), 414–419 (2004).
[25] Siggaard-Andersen, O., NÃrgaard-Pedersen, B., and Rem, J., "Hemoglobin pigments. spectrophotometric determination of oxy-, carboxy-, met-, and sulfhemoglobin in capillary blood," *Clinica Chimica Acta* **42**(1), 85 – 100 (1972).
[26] Yarynovska, I. H. and Bilyi, A. I., "Absorption spectra of sulfhemoglobin derivatives of human blood," in [*Optical Diagnostics and Sensing VI*], Cote, G. L. and Priezzhev, A. V., eds., **6094**, 1–6, SPIE (2006).
[27] Meinke, M., Müller, G., Helfmann, J., and Friebel, M., "Optical properties of platelets and blood plasma and their influence on the optical behavior of whole blood in the visible to near infrared wavelength range," *Journal of Biomedical Optics* **12**(1), 014024–014024 (2007).
[28] Kinnunen, M., Kauppila, A., Karmenyan, A., and Myllylä, R., "Effect of the size and shape of a red blood cell on elastic light scattering properties at the single-cell level," *Biomedical Optics Express* **2**(7), 1803–1814 (2011).
[29] Roggan, A., Friebel, M., Dörschel, K., Hahn, A., and Muller, G., "Optical properties of circulating human blood in the wavelength range 400-2500 nm," *Journal of Biomedical Optics* **4**(1), 36–46 (1999).
[30] Lindberg, L.-G. and Oberg, P. A., "Optical properties of blood in motion," *Optical Engineering* **32**(2), 253–257 (1993).
[31] Švejcar, J., Přerovskỳ, I., Linhart, J., and Kruml, J., "Content of collagen, elastin, and water in walls of the internal saphenous vein in man," *Circulation Research* **11**(2), 296–300 (1962).
[32] Bashkatov, A. N., Genina, E. A., and Tuchin, V. V., "Optical properties of skin, subcutaneous, and muscle tissues: a review," *Journal of Innovative Optical Health Sciences* **4**(01), 9–38 (2011).
[33] Butler, W. L., "Absorption spectroscopy in vivo theory and application," *Annual Review of Plant Physiology* **15**(1), 451–460 (1964).
[34] Latimer, P., "A wave-optics effect which enhances light absorption by chlorophyll *in vivo*," *Photochem. Photobiol.* **40**(2), 193–199 (1984).
[35] Natural Phenomena Simulation Group (NPSG), "Human Skin Data." http://www.npsg.uwaterloo.ca/data/skin.php (February 2017).
[36] Natural Phenomena Simulation Group (NPSG), "Human Blood Data." http://www.npsg.uwaterloo.ca/data/blood.php (February 2017).
[37] Roggan, A., Dorschel, K., Minet, O., Wolff, D., and Müller, G., "The optical properties of biological tissue in the near infrared wavelength range," *Laser-induced Interstitial Therapy. SPIE Press, Bellingham, WA* , 10–44 (1995).
[38] Baranoski, G. V. G., Rokne, J. G., and Xu, G., "Virtual spectrophotometric measurements for biologically and physically based rendering," *The Visual Computer* **17**(8), 506–518 (2001).
[39] Lister, T. S., *Simulating the Color of Port Wine Stain Skin*, PhD thesis, University of Southampton,U. K. (February 2013).
[40] Talreja, P. S., Kasting, G. B., Kleene, N. K., Pickens, W. L., and Wang, T., "Visualization of the lipid barrier and measurement of lipid pathlength in human stratum corneum," *AAPS PharmSci* **3**(2), 48–56 (2001).
[41] Magnenat-Thalmann, N., Kalra, P., L. Leveque, J., Bazin, R., Batisse, D., and Querleux, B., "A computational skin model: fold and wrinkle formation," *IEEE Transactions on Information Technology in Biomedicine* **6**(4), 317–323 (2002).
[42] Plewig, G., Scheuber, E., Reuter, B., and Waidelich, W., "Thickness of the corneocytes," in [*Stratum Corneum*], Marks, R. and Plewig, G., eds., 171–174, Springer-Verlag, Berlin (1983).

[43] Robertson, K. and Rees, J. L., "Variation in epidermal morphology in human skin at different body sites as measured by reflectance confocal microscopy," *Acta Derm. Venereol.* **90**, 368–373 (2010).
[44] Agache, P., "Metrology of the stratum corneum," in [*Measuring the Skin*], Agache, P. and Humbert, P., eds., 101–111, Springer-Berlag, Berlin, Germany (2004).
[45] Querleux, B., Darrasse, L., and Bittoun, J., "Magnetice resonance imaging of human skin in vivo," in [*Bioengineering of the Skin Skin Imaging and Analysis*], Wilhelm, K., Berardesca, E., Elsner, P., and Maibach, H. I., eds., 99–109, CRC Press, Boca Raton, FL, USA (2007).
[46] Robertson, K. and Rees, J. L., "Variation in epidermal morphology in human skin at different body sites as measured by reflectance confocal microscopy.," *Acta dermatovenereologica* **90**(4), 368–373 (2010).
[47] Shimizu, H., [*Shimizu's Textbook of Dermatology*], Hokkaido University Press (2007).
[48] Thody, A. J., Higgins, E. M., Wakamatsu, K., Ito, S., Burchill, S. A., and Marks, J. M., "Pheomelanin as well as eumelanin is present in human epidermis," *J Investig Dermatol* **97**, 340–344 (08 1991).
[49] Hennessy, A., Oh, C., Diffey, B., Wakamatsu, K., Ito, S., and Rees, J., "Eumelanin and pheomelanin concentrations in human epidermis before and after UVB irradiation," *Pigment Cell Research* **18**, 220–223 (2005).
[50] Noll, M. L. and Byers, J. F., "Usefulness of measures of Svo_2, Spo_2, vital signs, and derived dual oximetry parameters as indicators of arterial blood gas variables during weaning of cardiac surgery patients from mechanical ventilation," *Heart & Lung* **24**(3), 220–227 (1995).
[51] Lovell, A. T., Hebden, J. C., Goldstone, J. C., and Cope, M., "Determination of the transport scattering coefficient of red blood cells," in [*Proc. SPIE 3597, Optical Tomography and Spectroscopy of Tissue III*], *Proc. SPIE* **3597**, 175–182 (1999).
[52] Flewelling, R., "Noninvasive optical monitoring," in [*The Biomedical Engineering Handbook*], Bronzino, J. D., ed., CRC Press LLC, 2 ed. (2000).
[53] S. Haymond, R. Cariappa, C. S. E. and Scott, M. G., "Laboratory assessment of oxygenation in methemoglobinemia," *Clinical Chemistry* **51**(2), 434–444 (2005).
[54] Cunnington, A. J., Kendrick, S. F. W., Wamola, B., Lowe, B., and Newton, C. R. J. C., "Carboxyhemoglobin levels in Kenyan children with plasmodium falciparum malaria," *The American Journal of Tropical Medicine and Hygiene* **71**(1), 43–47 (2004).
[55] Rolinski, B., Küster, H., Ugele, B., Gruber, R., and Horn, K., "Total bilirubin measurement by photometry on a blood gas analyzer: Potential for use in neonatal testing at the point of care,," *Clinical Chemistry* **47**(10), 1845–1847 (2001).
[56] Lee, R., Mathews-Roth, M. M., Pathak, M. A., and Parrish, J. A., "The detection of carotenoid pigments in human skin," *J Investig Dermatol* **64**, 175–177 (03 1975).
[57] Agache, P. and Humbert, P., [*Measuring the Skin*], Springer (2004).
[58] Nakagawa, N., Matsumoto, M., and Sakai, S., "*In vivo* measurement of the water content in the dermis by confocal Raman spectroscopy," *Skin Research and Technology* **16**(2), 137–141 (2010).
[59] Viator, J. A., Komadina, J., Svaasand, L. O., Aguilar, G., Choi, B., and Stuart, N. J., "A comparative study of photoacoustic and reflectance methods for determination of epidermal melanin content," *Journal of Investigative Dermatology* **122**, 1432–1439 (06 2004).
[60] Williams, M. L., Hincenbergs, M., and Holbrook, K. A., "Skin lipid content during early fetal development," *Journal of Investigative Dermatology* **91**, 263–268 (09 1988).
[61] Squier, C. A., Cox, P., and Wertz, P. W., "Lipid content and water permeability of skin and oral mucosa," *Journal of Investigative Dermatology* **96**(1), 123–126 (1991).
[62] Cerussi, A. E., Berger, A. J., Bevilacqua, F., Shah, N., Jakubowski, D., Butler, J., Holcombe, R. F., and Tromberg, B. J., "Sources of absorption and scattering contrast for near-infrared optical mammography," *Academic radiology* **8**, 211–218 (March 2001).
[63] Fuchs, E., "Keratins and the skin," *Annual Review of Cell and Developmental Biology* **11**(1), 123–154 (1995).
[64] Gawkrodger, D. J., [*Dermatology An Illustrated Colour Text*], Churchill Livingstone (2002).
[65] Young, A. R., "Chromophores in human skin," *Phys. Med. Biol.* **42**(5), 789 (1997).

[66] Varcoe, J. S., [*Clinical Biochemistry: Techniques and Instrumentation : A Practical Course*], World Scientific (2001).
[67] Flindt, R., [*Amazing Numbers in Biology*], Springer (2006).
[68] Tearney, G. J., Brezinski, M. E., Southern, J. F., Bouma, B. E., Hee, M. R., and Fujimoto, J. G., "Determination of the refractive index of highly scattering human tissue by optical coherence tomography," *Opt. Lett.* **20**, 2258–2260 (Nov 1995).
[69] Diffey, B. L., "A mathematical model for ultraviolet optics in skin," *Physics in Medicine and Biology* **28**(6), 647–657 (1983).
[70] Tuchin, V. V., [*Tissue Optics: Light Scattering Methods and Instruments for Medical Diagnosis*], SPIE PM, SPIE/International Society for Optical Engineering (2007).
[71] Bashkatov, A. N., Genina, E. A., Kochubey, V. I., l M. Stolnitz, M., Bashkatova, T. A., Novikova, O. V., Peshkova, A. Y., and Tuchin, V. V., "Optical properties of melanin in the skin and skinlike phantoms," in [*Controlling Tissue Optical Properties: Applications in Clinical Study*], Tuchin, V. V., ed., **4162**(1), 219–226, SPIE (2000).
[72] Wang, X., Milner, T. E., and anf J. S. Nelson, M. C. C., "Group refractive index measurement of dry and hydrated type I collagen films using optical low-coherence reflectometry," *J. Biomed. Opt.* **12**, 212–216 (1996).
[73] Alaluf, S., Atkins, D., Barret, K., Blount, M., Carter, N., and Heath, A., "Ethnic variation in melanin content and composition in photoexposed and photoprotected human skin," *Pigment Cell Research* **15**, 112–118 (2002).
[74] Bain, B. J., Bates, I., Laffan, M. A., and Lewis, S. M., [*Dacie and Lewis Practical Haematology*], Elsevier Churchill Livingstone, 11 ed. (2012).
[75] Mokken, F. C., van der Waart, F. J. M., Henny, C. P., Goedhart, P. T., and Gelb, A. W., "Differences in peripheral arterial and venous hemorheologic parameters," *Annals of Hematology* **73**(3), 135–137 (1996).
[76] Kiray, A., Ergür, I., Tayefi, H., Bağriyanik, H. A., and Bacakoğlu, A. K., "Anatomical evaluation of the superficial veins of the upper extremity as graft donor source in microvascular reconstructions: a cadaveric study.," *Acta Orthopaedica et Traumatologica Turcica* **47**(6), 405–410 (2012).
[77] Klarhöfer, M., Csapo, B., Balassy, C., Szeles, J. C., and Moser, E., "High-resolution blood flow velocity measurements in the human finger," *Magnetic Resonance in Medicine* **45**(4), 716–719 (2001).
[78] Papaioannou, T. G. and Stefanadis, C., "Vascular wall shear stress: basic principles and methods," *Hellenic J Cardiol* **46**(1), 9–15 (2005).
[79] Yoxall, C. W. and Weindling, A. M., "Measurement of venous oxyhaemoglobin saturation in the adult human forearm by near infrared spectroscopy with venous occlusion," *Medical and Biological Engineering and Computing* **35**(4), 331–336 (1997).
[80] Yarynovska, I. H. and Bilyi, A. I., "Absorption spectra of sulfhemoglobin derivates of human blood," in [*Biomedical Optics 2006*], International Society for Optics and Photonics (2006).
[81] Haymond, S., Cariappa, R., Eby, C. S., and Scott, M. G., "Laboratory assessment of oxygenation in methemoglobinemia," *Clinical Chemistry* **51**(2), 434–444 (2005).
[82] Cunnington, A. J., Kendrick, S. F., Wamola, B., Lowe, B., and Newton, C. R. J. C., "Carboxyhemoglobin levels in Kenyan children with plasmodium falciparum malaria," *The American Journal of Tropical Medicine and Hygiene* **71**(1), 43–47 (2004).
[83] McCartney, E. J., [*Optics of the Atmosphere: Scattering by Molecules and Particles*], John Wiley & Sons (1976).
[84] Hunt, R. W. G., [*Measuring Colour*], Ellis Horwood Limited, Chichester, England, 2nd ed. (1991).
[85] Baranoski, G. V. G. and Krishnaswamy, A., [*Light & Skin Interactions: Simulations for Computer Graphics Applications*], Morgan Kaufmann/Elsevier, Burlington, MA, USA (2010).
[86] Natural Phenomena Simulation Group (NPSG), "Run HyLIoS Online." http://www.npsg.uwaterloo.ca/models/hylios.php (May 2017).
[87] Natural Phenomena Simulation Group (NPSG), "NPSGD Framework." http://www.npsg.uwaterloo.ca/models/npsgd_software.php (May 2017).
[88] Natural Phenomena Simulation Group (NPSG), "Run CLBlood Online." http://www.npsg.uwaterloo.ca/models/clblood.php (May 2017).